Neuron, Volume *58*

Supplemental Data

A Presynaptic Giant Ankyrin Stabilizes the NMJ through Regulation of Presynaptic Microtubules and Transsynaptic Cell Adhesion

Jan Pielage, Ling Cheng, Richard D. Fetter, Pete M. Carlton, John W. Sedat, and Graeme W. Davis

Pielage et al., Supplemental Figure 1

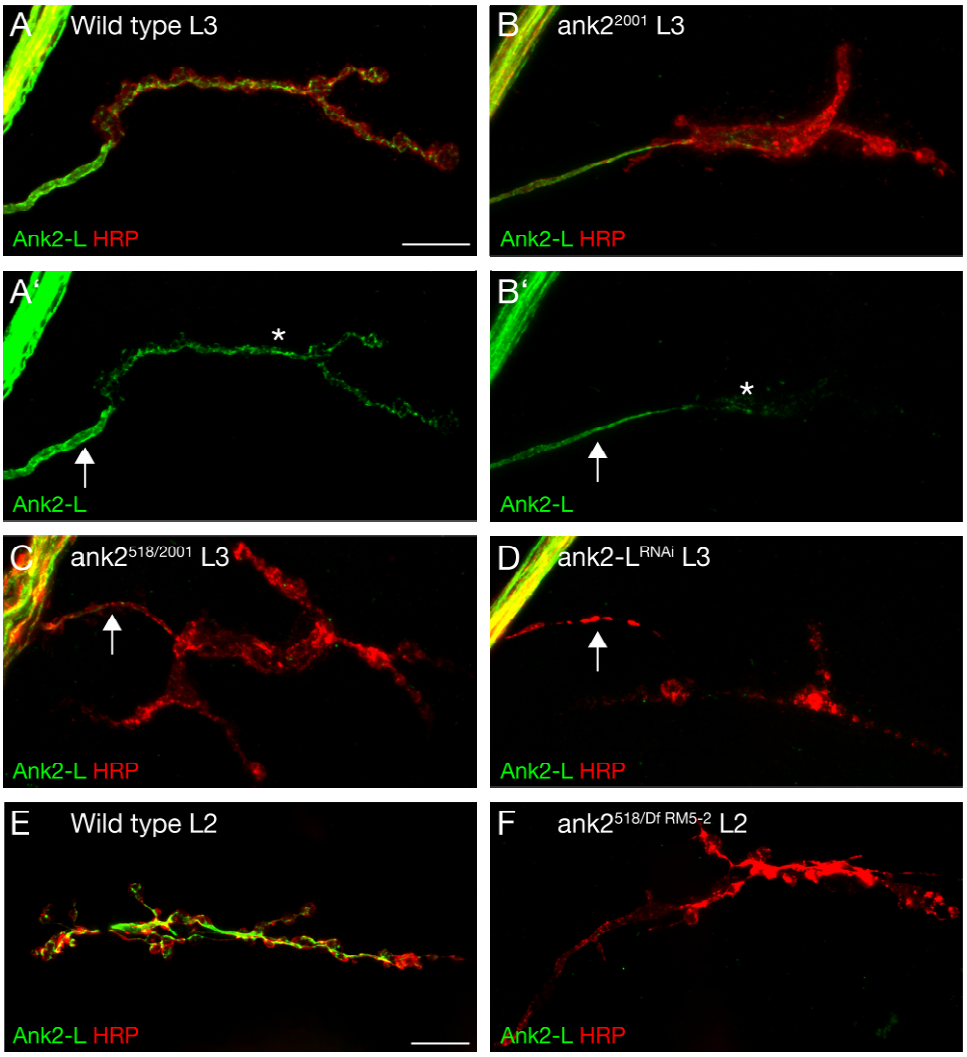

Supplemental Figure 1: Presynaptic Localization of Ank2-L is lost in *ank2* mutant animals. A, A') A wild type NMJ on muscle 4 stained with anti-Ank2-L (green) and the presynaptic membrane marker HRP (red). We observe high levels of Ank2-L in the motoneuron axon and within the presynaptic nerve terminal. Ank2-L shows a different localization in axons (arrow) compared to synaptic boutons (asterisk). **B, B'**) In animals homozygous for the transposon insertion $ank2^{2001}$ we observe a reduction in Ank2-L levels in the motoneuron axon (arrow) and almost a complete depletion of Ank2-L staining within the presynaptic nerve terminal (asterisk). **C**) In animals transheterozygous for the *ank2* mutations $ank2^{518/2001}$ Ank2-L immunoreactivity is nearly eliminated at the presynaptic nerve terminal and within the axon that extends form the main intersegmental nerve onto muscle 4 (arrow). **D**) Presynaptic expression of $ank2\text{-}L^{RNAi}$ results in an almost complete elimination of Ank2-L at the presynaptic nerve terminal and the axon that branches of the intersegmental nerve (arrow). However, Ank2-L staining remains in the intersegmental nerve. **E**) A second instar muscle 6/7 NMJ stained for Ank2-L and HRP. Ank2-L can be observed in the axons and all presynaptic boutons. **F**) In transheterozygous $ank2^{518/Df\ RM5\text{-}2}$ animals all Ank2-L immunoreactivity is lost in axons and synaptic boutons indicating that the $ank2^{518}$ mutation completely disrupts the *ank2-L* open reading frame. Scale bar in A-D and E, F 10 µm.

Pielage et al., Supplemental Figure 2

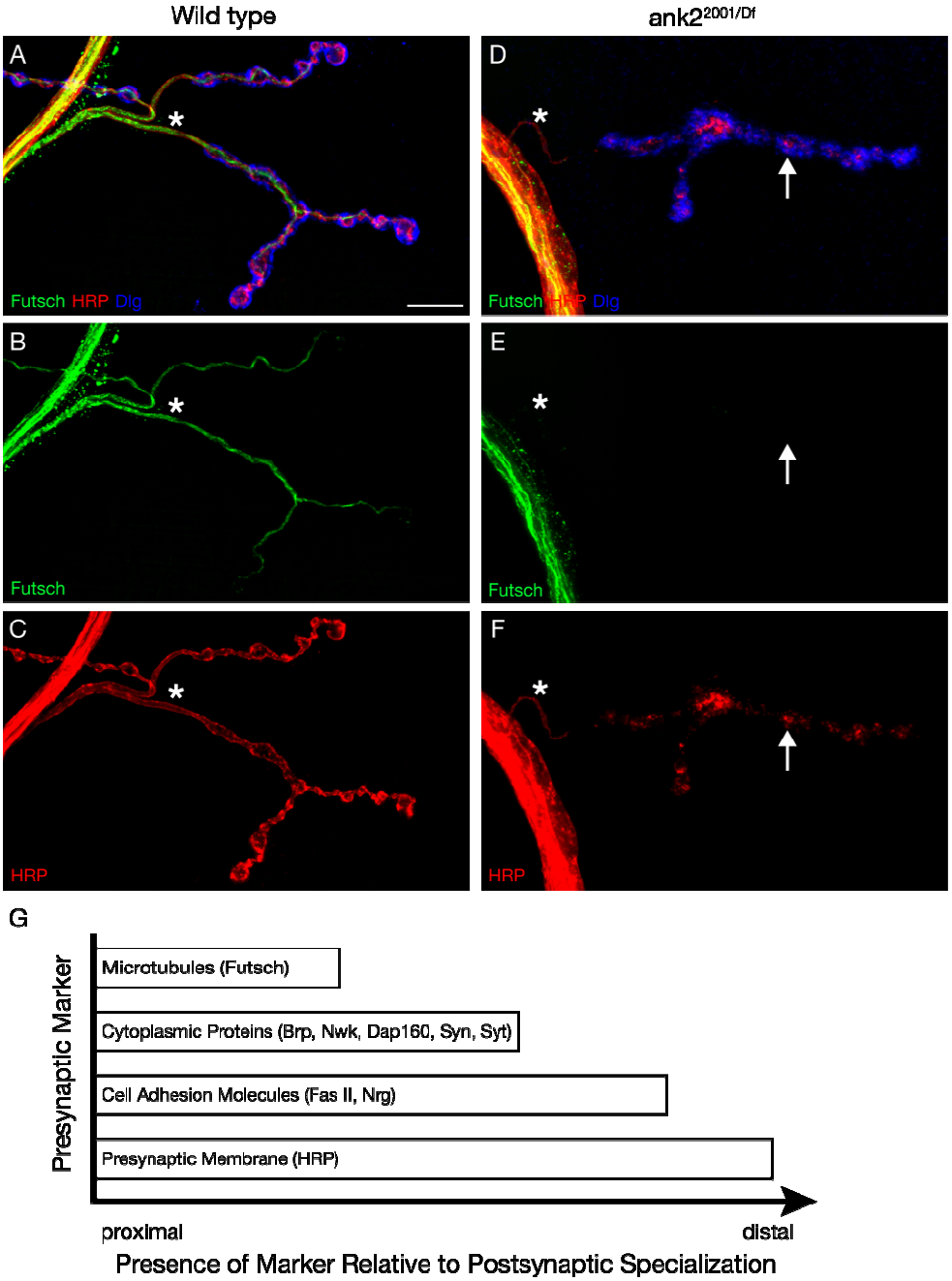

Supplemental Figure 2: Analysis of synaptic retractions in *ank2* mutant animals I. A-C) Wild type NMJ on muscle 4 stained for the microtubule-associated protein Futsch (green), the presynaptic membrane (HRP, red) and postsynaptic Dlg (blue). The Futsch-positive microtubules extend into all terminal boutons. **D-F**) *ank2*$^{2001/Df}$ mutant NMJ. Futsch staining is completely absent from the NMJ. Only fragmented remnants of the presynaptic membrane marked by HRP are still present opposite postsynaptic Dlg staining (arrow). The nerve ending prior to muscle innervation can still be detected but has a considerably smaller diameter (asterisk). **G**) Schematic of the sequence of disassembly events during the retraction of the NMJ. Scale bar in A-F 10 µm.

Supplemental Discussion for Supplemental Figure 2:

The schematic in Supplemental Figure 2 G summarizes our observations and suggests a sequential elimination of presynaptic markers during synapse retraction at the Drosophila NMJ. This schematic is not meant to imply that any of these proteins are required for synapse stability. Our data simply suggest a sequence of events, influenced by diverse factors including protein turnover and trafficking, that occur during the process of synapse retraction. This distinction is relevant when considering both the microtubule associated protein Futsch and the cell adhesion molecule Fas II. For example, Futsch is used as a marker to label the integrity of the presynaptic, bundled microtubule cytoskeleton (Roos et al., 2000). We previously demonstrated that hypomorphic *futsch*^{N94} mutations do not cause synapse retraction at the NMJ (Eaton and Davis, 2005). Null mutations in *futsch* are embryonic lethal. The hypomorphic *futsch*^{N94} mutant has been analyzed at the third instar NMJ (Roos et al., 2000; Eaton et al., 2005). We find that fragments of the microtubule cytoskeleton persist (Roos et al., 2000) and that both presynaptic Ank2-L as well as the synaptic cell adhesion molecule Fas II remain well organized (data not shown). Thus, the *futsch*^{N94} mutation does not recapitulate the molecular perturbations observed in *ank2-L* mutant animals and does not cause NMJ retraction. In contrast to *futsch* mutations *ank2-L* mutant animals not only lack Ank2-L protein but lead to a disruption of the synaptic microtubules and to a disruption of synaptic cell adhesion molecules including, but not limited to, Fas II. The same distinction also applies to the analysis of *fas II* mutations. As detailed in our text, *fas II* null mutations cause synapse retraction (Schuster et al., 1996). However, hypomorphic *fas II* mutations do not cause synapse retraction (Eaton et al., 2005). The hypomorphic *fas II* mutation decreases Fas II protein levels, however, both the neuronal cytoskeleton and other cell adhesion molecules persist (data not shown). Again, the loss of Ank2-L protein is a more severe, broad-spectrum perturbation.

Thus, to reiterate, the events diagrammed in Supplemental Figure 2 G simply depict the phenotypic sequence of events that occur at a retracting NMJ in *ank2* mutant animals. However, since a similar sequence of events has been reported in our prior publications examining mutations in other genes (Eaton et al., 2002; Pielage et al,. 2005) we hypothesize that this sequence of events may highlight a common sequence of events that occurs during NMJ retraction. This sequence of events may be strongly influenced by relative protein stability within the NMJ, by molecular scaffolds and by endogenous mechanisms of protein turnover.

Pielage et al., Supplemental Figure 3

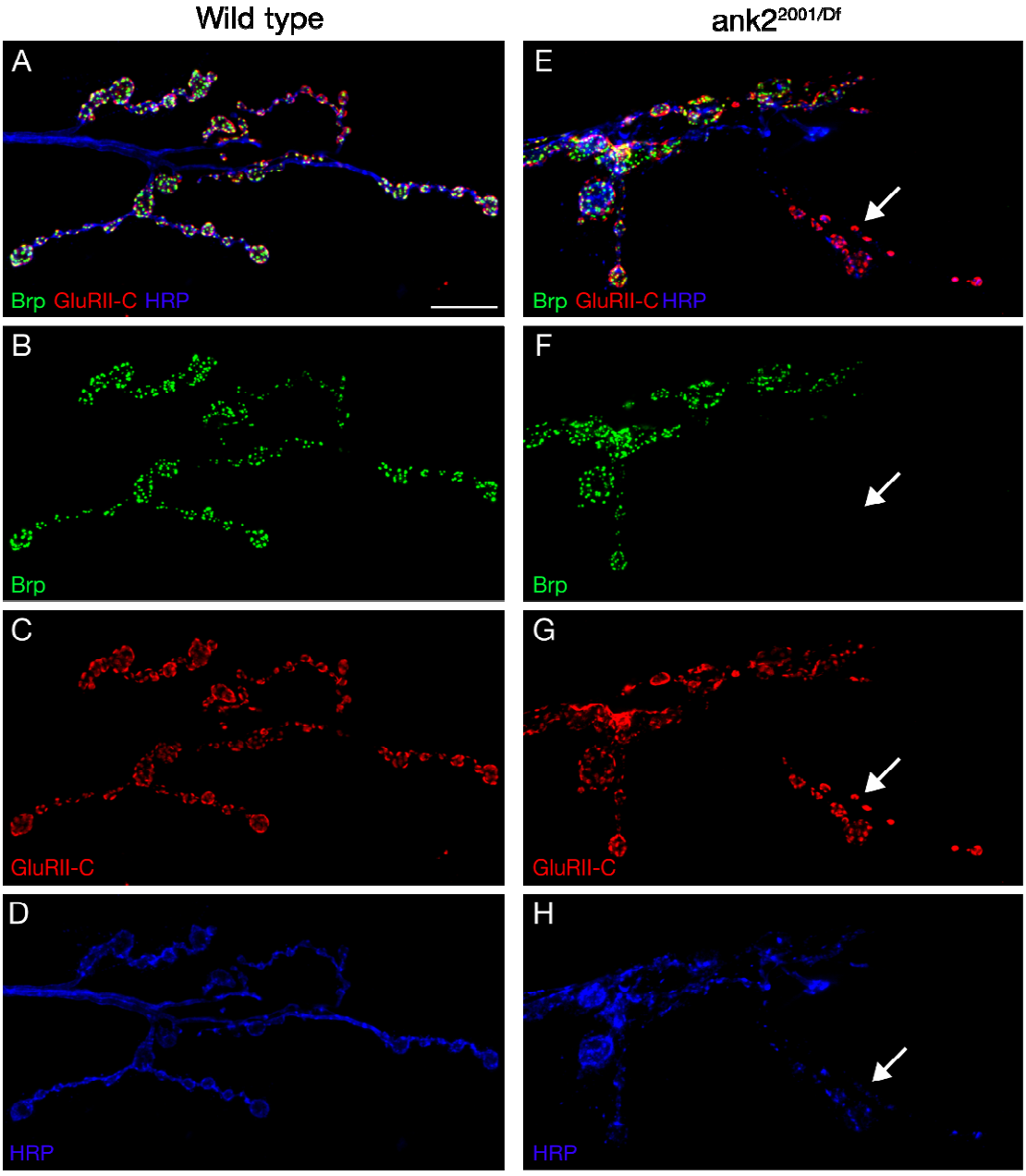

Supplemental Figure 3: Analysis of synaptic retractions in *ank2* mutant animals II. A-D) Wild type NMJ on muscle 6/7 stained for the presynaptic active zone protein Brp (green), the presynaptic membrane (HRP, blue) and postsynaptic glutamate receptor clusters (GluR-IIC, red). The active zone marker Brp is always found in perfect apposition to postsynaptic glutamate receptors. The presynaptic membrane is continuous throughout the NMJ. E-H) *ank2*$^{2001/Df}$ mutant NMJ. We observe regions within the NMJ where postsynaptic glutamate receptors are still clusters and present in normal abundance however the presynaptic active zone marker Brp is absent (arrow). At these sites the presynaptic membrane marker HPR is no longer continuous but becomes fragmented (H, arrow). Scale bar in A-H 10 µm.

Pielage et al., Supplemental Figure 4

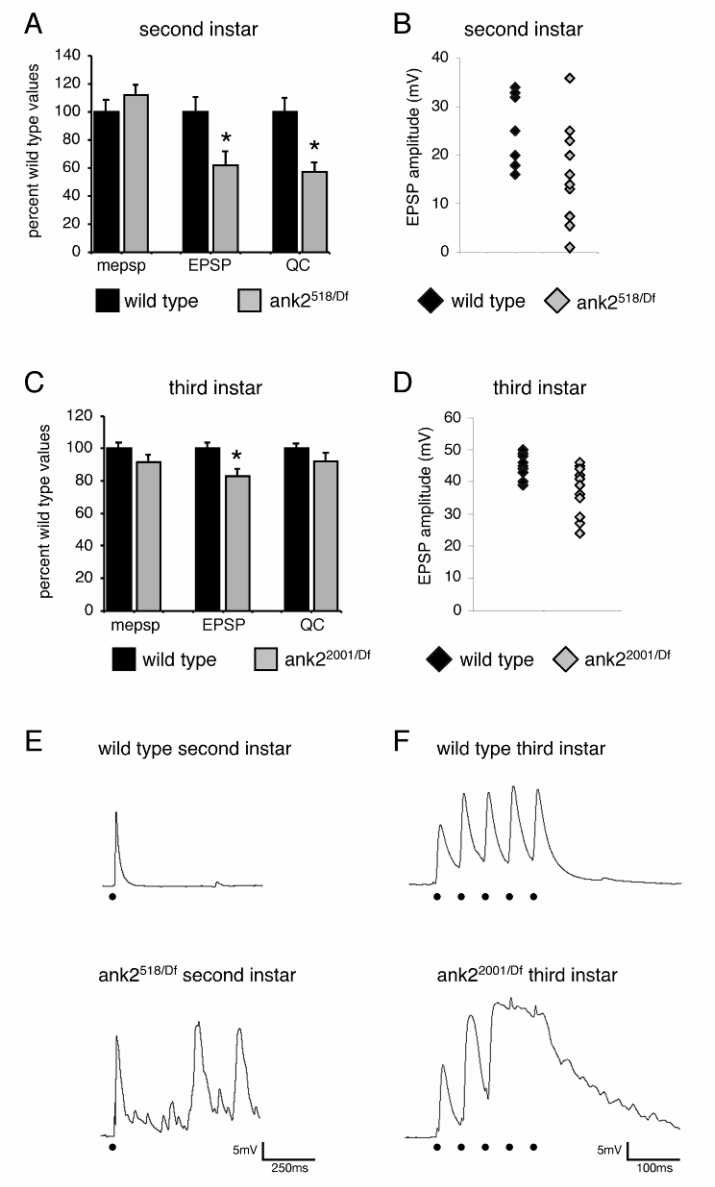

Supplemental Figure 4: Impaired evoked neurotransmission in *ank2* mutant animals. A, B) Analysis of neurotransmission in second instar wild type and *ank2*$^{518/Df\ RM5\text{-}2}$ animals. The loss of *ank2* results in impaired average evoked neurotransmission (EPSP) without affecting spontaneous miniature release events (mepsp). As a result we observe a significant decrease in the average quantal content (QC). **B**) Average EPSP amplitudes shown for each NMJ recording performed in the second instar *ank2*$^{518/Df\ RM5\text{-}2}$ animals. **C, D**) Analysis of synaptic transmission in third instar wild type and *ank2*$^{2001/Df\ RM5\text{-}2}$ animals. **E, F**) Loss of *ank2* results in hyper-excitability. **E**) A single stimulus (black circle) in wild type second instar animals reliably evokes a single EPSP. However, identical stimulation can evoke an extended presynaptic discharge, recorded postsynaptically as a large postsynaptic potential in *ank2*$^{518/Df\ RM5\text{-}2}$ animals. **F**) A train of 5 stimuli induces 5 EPSPs at the third instar NMJ of wild type animals. The same stimulation causes a large, abnormal, presynaptic discharge in *ank2*$^{2001/Df\ RM5\text{-}2}$ animals. Individual nerve stimuli are indicated by black circles.

Supplemental Discussion for Supplemental Figure 4:

We assayed synaptic function in *ank2-L* null mutant animals (*ank*^{f00518}/*Df(3L)RM5-2*) by recording from the NMJ of second instar larvae. We find no change in the amplitude of spontaneous miniature release events (mepsp), but observe a statistically significant decrease in both evoked neurotransmission (EPSP amplitude) and quantal content (QC; estimate of the number of vesicles released per action potential – see methods) (Supplemental Figure 4 A, B). This defect in neurotransmission varied considerably between NMJ recordings, with some NMJ functioning at nearly wild type levels while other NMJ showed almost a complete absence of evoked neurotransmission (Supplemental Figure 4 B). Based on our immunohistochemical analysis Ank2-L protein is completely eliminated from the NMJ in *ank*^{f00518}/*Df(3L)RM5-2* mutant animals (Supplemental Figure 1 F). Thus, the variability in the evoked neurotransmission most likely corresponds to the observed variability of NMJ degeneration in these animals. Since spontaneous neurotransmitter release and evoked neurotransmission can occur in the absence of Ank2-L protein, we conclude that Ank2-L is not required for vesicle release. We next assayed synaptic transmission in mutations that specifically disrupt only *ank2-L* (*ank2*^{2001}/*Df(3L)RM5-2*). These animals can survive to third instar stages and show evidence of NMJ degeneration (Figure 1 F, G). There is no significant change in the average mepsp amplitude. While we observe a significant decrease in the average EPSP amplitude there is no significant change in the average quantal content (Supplemental Figure 4 C, D).

An additional phenotype was also observed in these studies. We find that *ank2-L* mutant synapses are prone to hyper-excitability. The phenotype is strongest in the *ank*^{f00518}/*Df(3L)RM5-2* mutant animals where stimuli sufficient to evoke a single action potential in age matched wild type animals can now evoke long-lasting discharges that likely include numerous action potentials (Supplemental Figure 4 E). Although the severity of this phenotype is variable between recordings, we observe signs of hyper-excitability at ~80% of mutant synapses. This phenotype is never observed in wild type animals. A similar tendency toward hyper-excitability can be seen in homozygous *ank*^{2001} and in *ank2*^{2001}/*Df(3L)RM5-2* animals (Supplemental Figure 4 F). This phenotype of altered excitability is consistent with the ability of Ankyrins to bind and organize ion channels at the plasma membrane (Bennett and Baines, 2001).

Pielage et al., Supplemental Figure 5

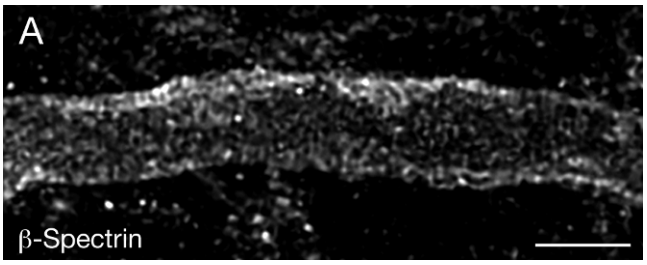

Supplemental Figure 5: Structured-illumination microscopy reveals a lattice-like organization of β-Spectrin in the axon. A) A wild type motoneuron axon stained for β-Spectrin. β-Spectrin is organized into a lattice-like pattern that contains pentameric and hexameric structures. Scale bar 2 µm.

Pielage et al., Supplemental Figure 6

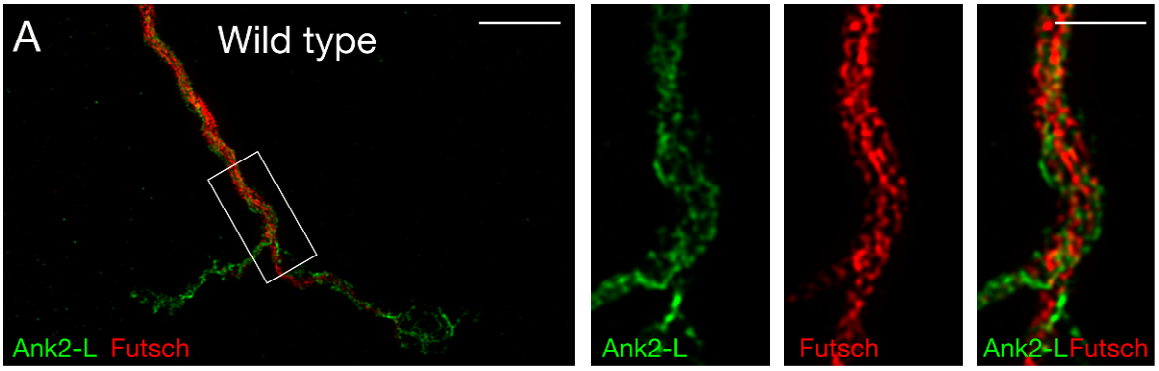

Supplemental Figure 6: Structured-illumination microscopy reveals a tight association between Ank2-L and the microtubule-associated protein Futsch. A) A wild type muscle 4 NMJ stained for Ank2-L (green) and the microtubule associated protein Futsch (red). Ank2-L is closely associated with Futsch staining. Scale bar in A 5 µm, insets 2 µm.

Pielage et al., Supplemental Figure 7

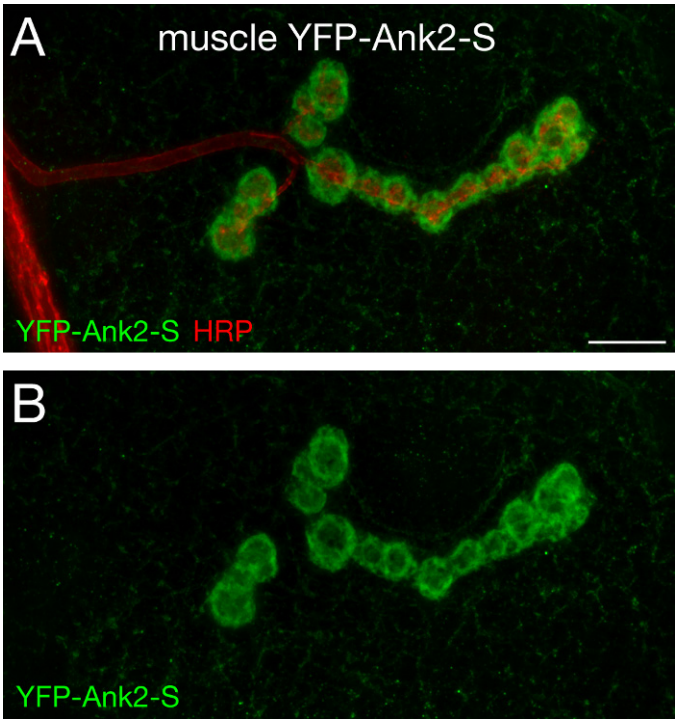

Supplemental Figure 7: The short isoform of Ank2 (Ank2-S) can localize to postsynaptic membranes. A, B) Muscle specific expression of YFP-Ank2-S leads to the accumulation of YFP-Ank2-S (green) in the postsynaptic membranes that surround the presynaptic boutons. Presynaptic boutons can be identified by the presynaptic membrane marker HRP (red). Scale bar in A-B 10 µm.

Pielage et al., Supplemental Methods:

RT-PCR of Ank2-L

The following primer pairs were used to verify the existence and expression of a continuous open reading frame connecting previously published *ank2* sequence to the novel exons previously annotated to encode *SP2523*. Positions are relative to the common ATG of all *ank2* isoforms. Connecting exon 9 (last shared exon between Ank2-S and Ank2-L) to exon 13 (within prior published sequence of *ank2b-e*; Hortsch et al., 2002). Pair 1 3207-3226: 5'-CCGCTTTGTCACCTACGACT□and 4662-4663: 5'-AGACTCCGATTCCTCGACCT. Pair 2 3207-3226: 5'-CCGCTTTGTCACCTACGACT□5612-5593: 5'-ATCGAGTCATCGCTTGGTTT. Connecting exon 13 to exon 17 (previously annotated as *SP2523*; includes stop codon). Pair 1 6247-6266: 5'-CTGAGCATGGAGCAACAAAA□and 7330-7311: 5'-ATTCTTTCGACGGTGGTACG. Pair 2 6802-6821: 5'-CAGCAACTGGCGAGTGAATA□and 8056-8037: 5'-GAGTTTCCGAGCCTTGTCTG. Pair 3 6507-6526: 5'-CTTGAGCATGGAGCAACAAA□and 7656-7637: 5'-CTCGTCCGTTTTGGAAATGT. DNA was amplified from a mixed staged embryonic cDNA library. All PCR-fragments were verified by sequencing. We detected multiple polymorphisms in the open reading frame compared to the published genomic sequence available at Flybase (www.flybase.org; Bloomington, Indiana). This open reading frame (*ank2-L*) corresponds to the transcript Ank2-RL and to the protein sequence Ank2-PL at Flybase.